

Visible-Light-Driven Selective Photocatalytic Hydrogenation of Cinnamaldehyde over Au/SiC Catalysts

Cai-Hong Hao,^{†,‡} Xiao-Ning Guo,^{*,†} Yung-Tin Pan,[§] Shuai Chen,[†] Zhi-Feng Jiao,^{†,‡} Hong Yang,^{*,§} and Xiang-Yun Guo^{*,†}

[†]State Key Laboratory of Coal Conversion, Institute of Coal Chemistry, Chinese Academy of Sciences, Taiyuan, Shanxi 030001, P. R. China

[‡]University of the Chinese Academy of Sciences, Beijing 100039, P. R. China

[§]Department of Chemical & Biomolecular Engineering, University of Illinois at Urbana–Champaign, 206 Roger Adams Laboratory, MC-712, 600 South Mathews Avenue, Urbana, Illinois 61801, United States

S Supporting Information

ABSTRACT: Highly selective hydrogenation of cinnamaldehyde to cinnamyl alcohol with 2-propanol was achieved using SiC-supported Au nanoparticles as photocatalyst. The hydrogenation reached a turnover frequency as high as 487 h⁻¹ with 100% selectivity for the production of alcohol under visible light irradiation at 20 °C. This high performance is attributed to a synergistic effect of localized surface plasmon resonance of Au NPs and charge transfer across the SiC/Au interface. The charged metal surface facilitates the oxidation of 2-propanol to form acetone, while the electron and steric effects at the interface favor the preferred end-adsorption of α,β -unsaturated aldehydes for their selective conversion to unsaturated alcohols. We show that this Au/SiC photocatalyst is capable of hydrogenating a large variety of α,β -unsaturated aldehydes to their corresponding unsaturated alcohols with high conversion and selectivity.

Selective hydrogenation of α,β -unsaturated aldehydes to unsaturated alcohols has attracted much attention recently because it is an essential step in the preparation of various fine chemicals.¹ An example is the reduction of cinnamaldehyde (CAL) to cinnamyl alcohol (COL), which is important for the synthesis of pharmaceuticals and perfumes.² Selective hydrogenation of CAL is often difficult, especially under heterogeneous catalysis conditions, because hydrogenation of C=C double bond is much more favorable than that of C=O double bond both thermodynamically and kinetically.³ Furthermore, when CAL adsorbs on metals, the competitive adsorption between C=C and C=O usually occurs.⁴ Significant efforts have been made in order to develop catalytic systems that are able to efficiently and selectively hydrogenate the C=O bond. Carefully designed self-assembled monolayers were used to ensure the preferred molecular configuration for hydrogenation of CAL to the desired product of COL.⁵ Electron-rich active sites were created on the catalyst surface to obtain high selectivity to COL.⁶ Such increase in surface electron density could not only enhance the repulsion between the active site and C=C bond, but also favor the C=O bond activation through favored back-bonding interaction between catalyst and

π^*_{CO} of CAL, thus higher selectivity toward the production of COL.⁷

In this Communication, we show SiC-supported Au nanoparticles (Au/SiC NPs) can be used as a new class of photocatalyst to selectively produce unsaturated alcohols from α,β -unsaturated aldehydes, including several important compounds as fragrance and flavor ingredients, such as, cinnamyl alcohol, crotyl alcohol, and 2-penten-1-ol. Au NPs absorb visible light strongly due to the localized surface plasmon resonance (LSPR) effect.^{8,9} Conduction electrons of Au NPs could be excited by visible light to become “hot”, which facilitate chemical reactions under mild conditions.¹⁰ Reductive coupling of nitroaromatic to azo compounds,¹¹ Suzuki–Miyaura cross-coupling¹² and oxidation of cyclohexane to cyclohexanone¹³ have all been realized through the light-driven processes using Au NPs. Even selective hydrogenation of organic compounds is also feasible by Au NP catalyst, though such application is often limited by the low H₂ activation. Cubic SiC (β -SiC), which is a semiconductor with a band gap of about 2.4 eV,¹⁴ absorbs visible light. SiC-supported Pd NPs were previously showed to have high photocatalytic activity for the hydrogenation of furan derivatives¹⁵ and Suzuki–Miyaura coupling reactions.¹⁶ Thus, SiC-supported Au NPs could be anticipated to exhibit excellent activity for selective hydrogenation of α,β -unsaturated aldehydes to unsaturated alcohols under visible light irradiation at ambient temperature.

Figure 1A shows the transmission electron microscopy (TEM) images of SiC-supported Au catalysts. The Au NPs are uniformly dispersed on the support and have an average diameter of 6.3 nm. β -SiC support, which has a BET specific surface area of 50 m²/g, was prepared by a sol–gel and carbothermal reduction method.¹⁷ The Au/SiC catalyst at a loading level of 1 wt% was prepared through the reduction of HAuCl₄. The formation of metallic Au was supported by the XRD patterns where the diffraction peaks for face-centered cubic Au metal are clearly visible (Figure S1A). Generally, the binding energy (BE) values of metallic Au are 84.0 eV for Au 4f_{7/2} and 87.7 eV for Au 4f_{5/2}.¹¹ The BE of Au particles in the Au/SiC catalyst shifted slightly to higher values, suggesting that

Received: April 23, 2016

Published: July 12, 2016

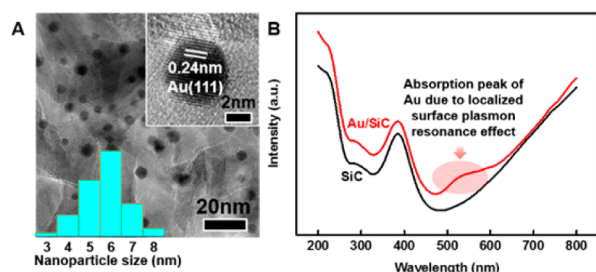


Figure 1. (A) TEM image and (B) UV-vis absorption spectra of the 1 wt% Au/SiC catalyst. The insets in (A) are the size distribution analysis and HRTEM image of Au NPs, respectively.

there existed electron-deficiency on Au particles (Figure S1B). Figure 1B shows the ultraviolet-visible (UV-vis) spectra of pure SiC and Au/SiC catalysts, respectively. The spectra indicate that β -SiC has strong UV and visible absorption. The strong absorption peak appearing at about 375 nm came from SiC, while the peak at approximately 520 nm could be attributed to the LSPR absorption of Au NPs. The absorption above 500 nm came mainly from the those of SiC and the reflection of sample in the measurement.

Performances of this Au/SiC photocatalyst for selective hydrogenation of CAL were conducted in an isopropyl alcohol solution under the irradiation of a 300-W Xe lamp whose wavelengths range from 400 to 800 nm. Hydrogenation reaction did not occur under light irradiation alone without the catalyst. The conversion of CAL was only 24% with a COL selectivity of 61% using only pure SiC under the same irradiation, suggesting SiC has moderate catalytic activity for the reaction. The Au/SiC catalyst, however, exhibited excellent photocatalytic performance under the same conditions. The conversion of CAL had a turnover frequency (TOF) as high as 487 h^{-1} , while the selectivity was 100% to the production of COL (Table 1, entry 1). This TOF value is the highest among the reported data so far (Table S1). Control experiments showed that no reaction occurred in the dark under identical conditions. When the light intensity was reduced from 1.0 to 0.9, 0.8, 0.7, 0.6, and 0.5 W/cm^2 (measured under the quartz window in the reactor) while all the other experimental conditions remained unchanged, the TOF linearly decreased from 487 to 423, 380, 309, 232, and 181 h^{-1} , respectively, indicating the reaction was driven by the light irradiation (Figure 2A). The reduced catalytic activity is likely due to the decrease in the number of activated electrons generated at low irradiation intensity. This linear relationship indicates the process should be first order in photon, suggesting that the reaction is dominated by a single photon absorption event.¹⁸

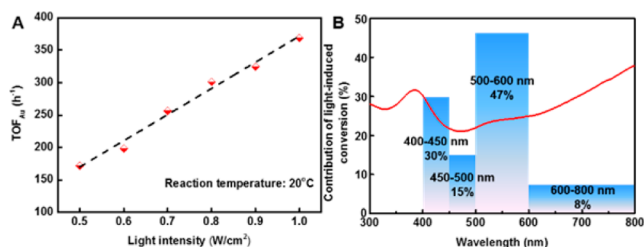


Figure 2. Dependence of catalytic activity of 1 wt% Au/SiC for the selective hydrogenation of CAL on the intensity (A) and wavelength (B) of the irradiation. The red line in (B) is the absorption spectrum of the catalyst.

Figure 2B shows the dependence of catalytic activity on the irradiation wavelength using the procedures similar to those reported in literatures.^{15,16,19} The conversion of CAL was 100% for the irradiation wavelength range of 400–800 nm, 70% for 450–800 nm, 55% for 500–800 nm and 8% for 600–800 nm. The COL selectivity however remained to be 100% regardless the range of wavelength. Since no reaction occurred without light, the light-induced conversion within each wavelength range was about 30% for 400–450 nm, 15% for 450–500 nm, 47% for 500–600 nm and 8% for 600–800 nm (Figure 2B). These values are consistent with the UV-vis absorption of the Au/SiC catalyst. The light absorption of SiC below 460 nm and the LSPR effect of Au nanoparticles in 500–600 nm contributed to the reaction the most. The near-infrared light from 600 to 800 nm appeared to have the smallest impact on the reaction.

For comparison, the performances of Au/TiO₂ and Au/Al₂O₃ catalysts with the same Au loading of 1 wt% were examined. The average size of Au NPs is 7.1 nm for Au/TiO₂ catalyst and 5.9 nm for Au/Al₂O₃ (Figure S2). No detectable conversion of CAL was observed over Al₂O₃, while the CAL conversion over TiO₂ was only 9% under the same irradiation. By loading Au NPs onto these supports, strong absorption was observed around 520 nm (Figure 3A), and the conversion of

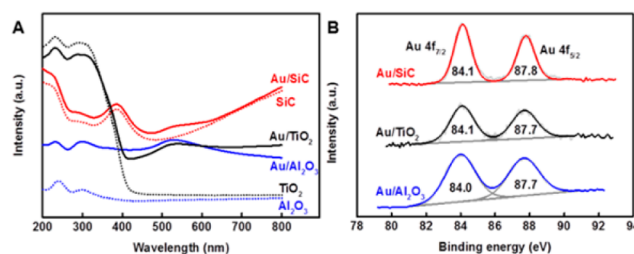


Figure 3. (A) UV-vis and (B) X-ray photoelectron spectra of Au/SiC, Au/TiO₂ and Au/Al₂O₃ catalysts and supports.

CAL increased remarkably to 47% over Au/Al₂O₃ and 73% over Au/TiO₂ under the same irradiation (400–800 nm) at 20 °C. Furthermore, if the reaction was conducted under UV irradiation (200–270 nm) with light intensity of 1.0 W/cm^2 , a nearly 100% conversion for CAL hydrogenation with 100% selectivity of COL was achieved for the Au/TiO₂ catalyst at 20 °C. This high performance is likely due to the interband transition of electrons in Au NPs. Without irradiation, no product was detected for either one of the two catalysts. Thus, the observed photocatalytic activity should be directly related to the LSPR effect of Au NPs at 400–800 nm,¹⁰ and the synergistic effect between Au and SiC support further enhance the conversion. While they require careful structural design, plasmonic metal/semiconductor photocatalysts can allow for the hot electrons transferring only from metal to semiconductor with the alignment between band levels of the semiconductor and Fermi level of the metal.^{10,20} Fast electron transfer from 10 nm gold nanodots to TiO₂ NPs was observed previously by using femtosecond transient absorption spectroscopy with an infrared probe.²¹ In our systems, the value of Au BE was found to be slightly higher in either Au/TiO₂ or Au/SiC than in Au/Al₂O₃ system (Figure 3B).

Thus, a visible light photon-induced catalytic process could contribute to the enhanced hydrogenation of CAL over the Au/SiC catalyst. In this model, the LSPR results in transition of electrons on six sp-hybridized orbitals of Au NPs to high energy levels.²² These electrons migrate to the conduction band of

SiC, leading to the formation of both slightly positively charged sites on Au NP and electron-rich sites at the interface between Au and SiC. In other words, there could exist a space charge region or built-in electric field at the Au/SiC interface due to the Mott–Schottky effect, and the light irradiation could promote the directional transfer of electrons.¹⁶ 2-Propanol can be oxidized on the relative positive sites on Au to generate acetone and active hydrogen. The latter reacts with the C=O bond of CAL to produce COL. Our results suggest that both electron and steric hindrance effects at the interface should be important, as those molecules with bulky ring structures show relatively high conversion and selectivity (see Table 1), most likely because they favor the adsorption of CAL molecules and the C=O bond at the end is adsorbed preferably on the active sites at the interface. Energy transferred from the LSPR dipole at Au/SiC interface via resonance should facilitate the charge separation, thus enhance the visible light-driven photocatalytic activity.²³

The Pd/SiC and Pt/SiC at 1 wt% catalyst loading were also studied (Figure S3) for the conversion of CAL. The conversion was 35% for Pd/SiC and 47% for Pt/SiC (Table S2). These results suggest that the photogenerated electrons mainly transfer from SiC to Pd or Pt through the Schottky–Mott contact,²⁴ and positively charged sites exist on the SiC surface for Pd/SiC or Pt/SiC. Accordingly, activated hydrogen species could be generated on SiC surface, and participate in the reaction.¹⁵ The appropriate direction of built-in electric field should be important for this reaction process. The selectivity for COL was high on both of these two catalysts, suggesting the active sites should still be at the metal/SiC interface.

We quantified the thermodynamic parameters for the hydrogenation of CAL in the temperature range between 30 and 70 °C under irradiation and in the dark. The apparent activation energy was calculated to be 35.1 kJ/mol under irradiation (400–800 nm) and 85.8 kJ/mol in the dark, based on the Arrhenius equation. The large difference in activation energy suggests the reaction mechanisms with and without light irradiation should be very different. The former process (with light) is mainly driven by charge carrier. The electrons generated due to LSPR activate the adsorbates to form excited states and move to a different potential energy surface to take part in the reaction.¹⁰ The latter process (without light) is mainly driven by the phonon effect. The thermal energy results in the reactant adsorbates to move to the ground-state potential energy surface of the product.¹⁰ Thus, the TOF values should increase with temperature with or without irradiation, but at different efficiency (Figure 4A). Since elevated temperature can not only increase the population of reactant molecules in excited states, but also cause a redistribution of the conduction

electrons on Au NPs into higher energy levels. The linear dependence of enhancement in activity on the intensity of light indicates that the photoexcitation of the energized electrons and LSPR are the primary factors responsible for the observed enhanced photocatalytic activity (Figure 4B).²⁵

Besides CAL, a variety of other α,β -unsaturated aldehydes were studied under the optimized conditions, and the results are summarized in Table 1. All the α,β -unsaturated aldehydes

Table 1. Selective Photocatalytic Hydrogenation of α,β -Unsaturated Aldehydes over Au/SiC Catalyst^a

Entry	Reactant	Main product	Conv.(%)	Select.(%) ^b	TOF _{Au} (h ⁻¹)
1			100	100	487
2			85	92	205
3			100	93	122
4			81	100	106
5			100	100	263
6			90	93	220
7			92	96	233
8			77	89	180
9			70	84	155
10			72	85	161
11			64	81	136
12			53	72	100

^aReaction conditions: 1.6 mmol of reactant, 30 mg of 1 wt% Au/SiC catalyst in 10 mL of isopropyl alcohol containing of 20 mg of KOH. The reactions were conducted under an argon atmosphere at 20 °C under Xe lamp irradiation (400–800 nm) with light intensity of 1.0 W/cm². The reaction time was 4 h, except for entry 1 (130 min) and entries 3 and 4 (8 h). ^bAmong the other compounds generated, saturated aldehydes and saturated alcohols were the main products.

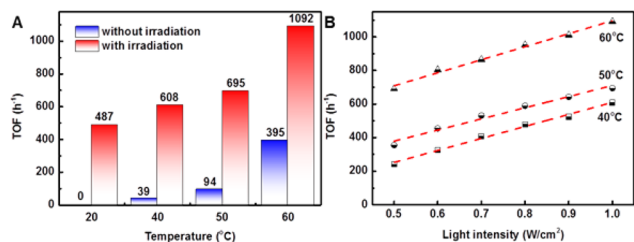


Figure 4. TOF of hydrogenation of cinnamaldehyde over Au/SiC catalysts as a function of (A) temperature with and without irradiation (1.0 W/cm²) and (B) light intensity at various temperatures.

tested showed photoinduced selective hydrogenation over the Au/SiC catalyst with high selectivity toward the production of corresponding unsaturated alcohols. Aromatic unsaturated aldehydes (entries 1–7) typically exhibited higher activity than the aliphatic unsaturated aldehydes (entries 8–10), likely due to the difference in the conjugation effects from the unsaturated carbon bonds.^{3b} Finally, Au/SiC catalysts also exhibited good activity for selective hydrogenation of α,β -unsaturated ketones (entries 11 and 12).

A main advantage of heterogeneous catalyst lies in its good stability, recyclability and ease in separation.²⁶ We investigated the recyclability of Au/SiC photocatalyst by reusing it after the process for up to five cycles under the same reaction condition. Comparing with the first one, the catalyst did not show

measurable loss in catalytic activity in the following four cycles after the initial run (Figure S4A), suggesting the excellent stability of this catalyst. TEM micrographs taken with the catalyst after the fifth catalytic cycle did not show obvious change in morphology and aggregation of Au NPs (Figure S4B). The XPS results show the Au NPs on the SiC support remained to be metallic and did not degrade in composition (Figure S4C).

In summary, we show that Au/SiC catalyst can effectively utilize visible light in selective hydrogenation of α,β -unsaturated aldehydes to corresponding unsaturated alcohols (such as CAL to COL) with high TOF and selectivity. The synergistic effect of LSPR on Au NPs with the charge separation property at the Au/SiC interface is critically important. The cooperative effects include the oxidation of 2-propanol to generate acetone and active hydrogen when light-driven, and preferred adsorption of C=O end-group at the interface for reaction with hydrogen to produce alcohol due to LSPR-activated Au. The Au/SiC photocatalyst can be applied to selective hydrogenation of a range of α,β -unsaturated aldehydes to corresponding unsaturated alcohols, including many important, industrially relevant compounds. The scheme developed in this study should have broad ramifications in the design of semiconductor-supported plasmonic metal nanoparticle systems as photocatalysts for a wide range of organic transformations driven by light.

■ ASSOCIATED CONTENT

Supporting Information

The Supporting Information is available free of charge on the ACS Publications website at DOI: 10.1021/jacs.6b04175.

Details of preparations, characterizations (TEM micrographs, XPS data, etc.), studies of photocatalytic property, and data analysis (PDF)

■ AUTHOR INFORMATION

Corresponding Authors

*hy66@illinois.edu

*guoxiaoning@sxicc.ac.cn

*xyguo@sxicc.ac.cn

Notes

The authors declare no competing financial interest.

■ ACKNOWLEDGMENTS

The work was financially supported by NSFC (21403270 and 21473232), Shanxi Province (20131101035), SKLCC (2014BWZ006 and J15-16-909), and Youth Innovation Promotion Association (20131115). Y.-T.P. is grateful for a Dow Fellowship from UIUC.

■ REFERENCES

- (1) (a) Margitfalvi, J. L.; Tompos, A.; Kolosova, I.; Valyon, J. *J. Catal.* **1998**, *174*, 246. (b) Mitsudome, T.; Kaneda, K. *Green Chem.* **2013**, *15*, 2636.
- (2) (a) Vriamont, C.; Haynes, T.; McCague-Murphy, E.; Pennetreau, F.; Riant, O.; Hermans, S. *J. Catal.* **2015**, *329*, 389. (b) Rong, H. P.; Niu, Z. Q.; Zhao, Y. F.; Cheng, H.; Li, Z.; Ma, L.; Li, J.; Wei, S. Q.; Li, Y. D. *Chem. - Eur. J.* **2015**, *21*, 12034.
- (3) (a) Wang, Y. Y.; He, W. H.; Wang, L. R.; Yang, J. J.; Xiang, X.; Zhang, B.; Li, F. *Chem. - Asian J.* **2015**, *10*, 1561. (b) Shi, J. J.; Zhang, M. Y.; Du, W. C.; Ning, W. S.; Hou, Z. Y. *Catal. Sci. Technol.* **2015**, *5*, 3108.
- (4) Ponec, V. *Appl. Catal., A* **1997**, *149*, 27.

- (5) (a) Kahsar, K. R.; Schwartz, D. K.; Medlin, J. W. *J. Am. Chem. Soc.* **2014**, *136*, 520. (b) Vu, K. B.; Bukhryakov, K. V.; Anjum, D. H.; Rodionov, V. O. *ACS Catal.* **2015**, *5*, 2529. (c) Wu, B. H.; Huang, H. Q.; Yang, J.; Zheng, N. F.; Fu, G. *Angew. Chem., Int. Ed.* **2012**, *51*, 3440.
- (6) (a) Ma, H. X.; Wang, L. C.; Chen, L. Y.; Dong, C.; Yu, W. C.; Huang, T.; Qian, Y. T. *Catal. Commun.* **2007**, *8*, 452. (b) Wang, Y.; Rong, Z. M.; Wang, Y.; Zhang, P.; Wang, Y.; Qu, J. P. *J. Catal.* **2015**, *329*, 95. (c) Castillejos, E.; Debouttière, P. J.; Roiban, L.; Solhy, A.; Martinez, V.; Kihn, Y.; Ersen, O.; Philippot, K.; Chaudret, B.; Serp, P. *Angew. Chem., Int. Ed.* **2009**, *48*, 2529.
- (7) Delbecq, F.; Sautet, P. *J. Catal.* **1995**, *152*, 217.
- (8) (a) Linic, S.; Christopher, P.; Ingram, D. B. *Nat. Mater.* **2011**, *10*, 911. (b) Marimuthu, A.; Zhang, J.; Linic, S. *Science* **2013**, *339*, 1590. (c) Naya, S.; Niwa, T.; Kume, T.; Tada, H. *Angew. Chem., Int. Ed.* **2014**, *53*, 7305.
- (9) Bian, Z. F.; Tachikawa, T.; Zhang, P.; Fujitsuka, M.; Majima, T. *J. Am. Chem. Soc.* **2014**, *136*, 458.
- (10) Linic, S.; Aslam, U.; Boerigter, C.; Morabito, M. *Nat. Mater.* **2015**, *14*, 567.
- (11) Zhu, H. Y.; Ke, X. B.; Yang, X. Z.; Sarina, S.; Liu, H. W. *Angew. Chem., Int. Ed.* **2010**, *49*, 9657.
- (12) Sarina, S.; Zhu, H. Y.; Jaatinen, E.; Xiao, Q.; Liu, H. W.; Jia, J. F.; Chen, C.; Zhao, J. *J. Am. Chem. Soc.* **2013**, *135*, 5793.
- (13) Liu, R. H.; Huang, H.; Li, H. T.; Liu, Y.; Zhong, J.; Li, Y. Y.; Zhang, S.; Kang, Z. H. *ACS Catal.* **2014**, *4*, 328.
- (14) van Dorp, D. H.; Hijnen, N.; Di Vece, M.; Kelly, J. J. *Angew. Chem., Int. Ed.* **2009**, *48*, 6085.
- (15) Jiao, Z. F.; Guo, X. N.; Zhai, Z. Y.; Jin, G. Q.; Wang, X. M.; Guo, X. Y. *Catal. Sci. Technol.* **2014**, *4*, 2494.
- (16) Jiao, Z. F.; Zhai, Z. Y.; Guo, X. N.; Guo, X. Y. *J. Phys. Chem. C* **2015**, *119*, 3238.
- (17) Jin, G. Q.; Guo, X. Y. *Microporous Mesoporous Mater.* **2003**, *60*, 207.
- (18) Kale, M. J.; Avanesian, T.; Christopher, P. *ACS Catal.* **2014**, *4*, 116.
- (19) (a) Guo, X. N.; Hao, C. H.; Jin, G. Q.; Zhu, H. Y.; Guo, X. Y. *Angew. Chem., Int. Ed.* **2014**, *53*, 1973. (b) Guo, X. N.; Jiao, Z. F.; Jin, G. Q.; Guo, X. Y. *ACS Catal.* **2015**, *5*, 3836.
- (20) (a) Tian, Y.; Tatsuma, T. *J. Am. Chem. Soc.* **2005**, *127*, 7632. (b) Qian, K.; Sweeny, B. C.; Johnston-Peck, A. C.; Niu, W. X.; Graham, J. O.; DuChene, J. S.; Qiu, J. J.; Wang, Y. C.; Engelhard, M. H.; Su, D.; Stach, E. A.; Wei, W. D. *J. Am. Chem. Soc.* **2014**, *136*, 9842. (c) Zhang, Z.; Yates, J. T. *Chem. Rev.* **2012**, *112*, 5520.
- (21) Du, L. C.; Furube, A.; Hara, K.; Katoh, R.; Tachiya, M. *J. Photochem. Photobiol., C* **2013**, *15*, 21.
- (22) Sarina, S.; Waclawik, E. R.; Zhu, H. Y. *Green Chem.* **2013**, *15*, 1814.
- (23) Cushing, S. K.; Li, J. T.; Meng, F. K.; Senty, T. R.; Suri, S.; Zhi, M. J.; Li, M.; Bristow, A. D.; Wu, N. Q. *J. Am. Chem. Soc.* **2012**, *134*, 15033.
- (24) Li, X. H.; Antonietti, M. *Chem. Soc. Rev.* **2013**, *42*, 6593.
- (25) (a) Huang, X. Q.; Li, Y. J.; Chen, Y.; Zhou, H. L.; Duan, X. F.; Huang, Y. *Angew. Chem., Int. Ed.* **2013**, *52*, 6063. (b) Sarina, S.; Zhu, H. Y.; Xiao, Q.; Jaatinen, E.; Jia, J. F.; Huang, Y. M.; Zheng, Z. F.; Wu, H. S. *Angew. Chem., Int. Ed.* **2014**, *53*, 2935.
- (26) Schlögl, R. *Angew. Chem., Int. Ed.* **2015**, *54*, 3465.